B-spline-based complex-rotation method with spin-dependent interaction

T. K. Fang[1,*] and T. N. Chang[2,3]
[1]*Department of Physics, Fu Jen Catholic University, Taipei, Taiwan 242, Republic of China*
[2]*Department of Physics and Astronomy, University of Southern California, Los Angeles, California 90089-0484, USA*
[3]*National Center of Theoretical Sciences, Hsinchu, Taiwan 30039, Republic of China*
(Received 19 July 2006; revised manuscript received 2 January 2007; published 31 July 2007)

We present a *B*-spline-based complex-rotation (BSCR) method with spin-dependent interaction for the study of atomic photoionization leading to multiple ionization channels dominated by doubly excited resonances for two-electron and divalent atoms. The degree of mixing between different spin states and between the bound and continuum components of the state function of the resonance state can be easily identified in the BSCR method. Its application to Mg photoionization gives good agreement with observed singlet-triplet mixed Mg spectra.

DOI: 10.1103/PhysRevA.76.012721 PACS number(s): 32.80.Fb, 32.80.Dz, 32.70.Jz

I. INTRODUCTION

Recent applications of *B*-spline-based methods to the continuum, e.g., the *B*-spline-based configuration-interaction (BSCI) method for a single continuum [1] and the *B*-spline-based *K*-matrix (BSK) method for multiple continua [2,3], have shown the effectiveness of such methods for the study of doubly excited resonances for two-electron and divalent atoms [2,4]. A straightforward application of these two methods requires rapidly increasing computational effort as the number of ionization channels increases. Alternatively, using a complex scaled Hamiltonian with a set of *B*-spline-based orbital functions, Fang and Ho [5] have recently applied the complex-rotation method successfully to study the effects of an electric field on the structure profiles of doubly excited resonances in He.

Much earlier, Rescigno and McCurdy [6] employed a set of complex basis functions to reduce the problem of identifying resonances to the solution of a complex eigenvalue problem. In particular, Rescigno [7] applied the methods of complex basis functions to study in detail the lowest ^1P resonance for Mg. More recently, McCurdy and co-workers [8] have made substantial progress by using exterior complex scaling (ESC) to treat the atomic and molecular collision problem. In particular, they employed the *B*-spline [9] and other techniques to substantially reduce the computational effort (e.g., two-electron integrals with *B* splines under ESC) required in the application to atomic and molecular processes [10]. *B*-spline approaches for atomic and molecular processes have also been reviewed recently by Bachau *et al.* [11], including details on many of the earlier works by Chang and co-workers. Other recent *B*-spline works include a complex scaled application to photodetachment carried out by Sanz-Vicario *et al.* [12] and application to multiphoton processes by Nikolopoulos [13].

Instead of using a complex scaled Hamiltonian [14], Fang and co-workers [15] recently employed a set of complex *B*-spline-based basis functions to study the ^1P Mg resonance structure above the $3p\ ^2P$ threshold. The results of this preliminary *B*-spline-based complex-rotation (BSCR) application are in good agreement with the observed photoabsorption spectrum and the results of an earlier BSK calculation [15]. In Sec. II, we present a more comprehensive discussion of the BSCR method by including explicitly the spin-dependent interactions which account for the mixing of resonances corresponding to different spin states. In contrast to the BSK method, which can be applied to calculate directly the partial cross section for each ionization channel, the BSCR method, which requires substantially less computational effort, is limited to the calculation of total cross sections only. We should also note that the BSCR method could include the spin-dependent interactions substantially more easily than the BSK calculations. Instead of applying the *B*-splines directly (which are more efficient computationally), the orthonormal sets of atomic orbitals ae used in the BSCR calculation to facilitate an unambiguous identification of the dominating electronic configuration, and the mixing of the spin states for each doubly excited resonance.

In Sec. III, we present an application of the BSCR method to Mg ground-state photoionization, which leads to cross sections in good agreement with the observed Mg singlet-triplet mixed spectrum. The Mg photoabsorption spectrum, with two distinct autionization series (one narrow and one broad and separated from each other), offers a unique opportunity to study in detail the mixing of different spin states due to the relatively small, but nevertheless experimentally resolved, spin-dependent interactions. With the spin-dependent interactions explicitly included in the BSCR calculation, a small mixing of $3p^2\ ^3P_{J=0}$ in the ground state leads to the presence of $3pnd\ ^3D_{J=1}$ resonances in the photoionization spectrum. The photoionization spectra from the Mg metastable $3s4s\ ^3S_{J=1}$ state to $J=0,1,2$ continua are also presented.

II. THEORY

Similarly to the BSCI and BSK methods, the BSCR method also starts with a quasicomplete set of discretized one-particle functions $\chi_{nl}(r)$, corresponding to electronic orbitals nl with an orbital angular momentum l but variable energy (both negative and positive), defined by an effective one-particle Hamiltonian h_l^{eff}, i.e.,

*phys2018@mails.fju.edu.tw

$$h_l^{eff}\chi_{nl} = \epsilon_{nl}\chi_{nl}, \tag{1}$$

with a boundary condition $\chi_{nl}(r=R)=0$. A set of N B splines $B_{i,K}(r)$ of order K [9] is defined inside a sphere of radius R. The solution χ_{nl} is expanded as

$$\chi(r) = \sum_i^N C_i B_i(r), \tag{2}$$

where the index K is dropped for simplicity. The computational procedure used to generate the one-particle radial function $\chi(r)$ is given in detail in [1].

The Hamiltonian matrix is constructed with a set of J-dependent basis functions $\psi^{\Omega}_{n_1 l_1, n_2 l_2, \ldots}(\vec{r}_1, \vec{r}_2, \ldots)$ characterized by an electronic configuration $(n_1 l_1, n_2 l_2, \ldots)$ and a set of quantum numbers $\Omega \equiv (SLJM_J)$, where S, L, J, and M_J are the total spin, the total orbital angular momentum, the total angular momentum, and its corresponding magnetic quantum number, respectively. The basis function $\psi^{\Omega}_{n_1 l_1, n_2 l_2, \ldots}$ represents a sum of J-independent basis function $\psi^{\Lambda}_{n_1 l_1, n_2 l_2, \ldots}$ over all M_S and M, where $\Lambda \equiv (SLM_S M)$ is a set of quantum numbers S, L, M_S, and M. M_S and M are the magnetic quantum numbers of S and L, respectively. Within the central field approximation, the basis function $\psi^{\Lambda}_{n_1 l_1, n_2 l_2, \ldots}$ is expressed as a sum of Slater determinant wave functions corresponding to the configuration $(n_1 l_1, n_2 l_2, \ldots)$ over all magnetic quantum numbers with an appropriate angular momentum coupling. The Slater determinant wave functions are constructed in the usual form as the product of one-particle orbitals $\chi_{nl}(r)$. More details are given elsewhere [1].

In the BSCR method, the radial function representing an outgoing ionized $\varepsilon\ell$ electron of an open channel $n_o \ell_o \varepsilon \ell$, leaving the inner electron in an $n_o \ell_o$ orbital of the residue ion, is replaced by a complex function, i.e., the radius r is replaced by a complex variable $z = re^{-i\theta}$,

$$\chi_{\varepsilon\ell}(re^{-i\theta}) = \sum_{i=1}^N C_i^{\varepsilon\ell} B_i(re^{-i\theta}). \tag{3}$$

By staying with the real knot sequence in our calculation, the BSCR method differs from the ESC approach of McCurdy and co-workers, which uses a complex knot sequences [8]. In addition, a variational parameter β for each open channel is also introduced to define a modified complex radial function, i.e.,

$$\tilde{\chi}_{\varepsilon\ell}(z) = \sum_{i=1}^N C_i^{\varepsilon\ell} \tilde{B}_i(z), \tag{4}$$

where $\tilde{B}_i = B_i(z)e^{-\beta z}$. In other words, an open channel $|n_o \ell_o \varepsilon \ell(\theta, \beta)\rangle$ is represented by a set of complex nonorthogonal basis functions $\psi^{\Omega}_{n_o \ell_o \varepsilon \ell(\theta,\beta)}$. For a closed channel $|n_o \ell_o n \ell\rangle$, however, the radial functions $\chi_{n\ell}$ in a set of orthogonal basis functions $\psi^{\Omega}_{n_o \ell_o n\ell}$ remain real. In essence, the BSCR method employs a real Hamiltonian and real basis functions for all closed channels, but sets of back-rotated complex functions for open channels, similar to the method used by Davis and Chung [16].

Within the Breit-Pauli approximation [17], the Hamiltonian is given by

$$H = H_{nr} + H_m, \tag{5}$$

where H_{nr} is the N-electron nonrelativistic Hamiltonian given explicitly by Eq. (2) of [1] and H_m is the sum of spin-dependent interactions in Rydberg units, i.e.,

$$H_m = \alpha^2(H_{so} + H_{ss} + H_{soo}), \tag{6}$$

where α is the fine-structure constant,

$$H_{so} = \sum_i^N \frac{Z}{r_i^3}(\vec{\ell}_i \cdot \vec{s}_i) \tag{7}$$

is the spin-orbit interaction subject to a nuclear charge Z,

$$H_{ss} = \sum_{i\neq j}^N \frac{1}{r_{ij}^3}\left(\vec{s}_i \cdot \vec{s}_j - 3\frac{(\vec{s}_i \cdot \vec{r}_{ij})(\vec{s}_j \cdot \vec{r}_{ij})}{r_{ij}^2}\right) \tag{8}$$

is the spin-spin interaction,

$$H_{soo} = \sum_{i\neq j}^N \frac{1}{r_{ij}^3}(\vec{r}_{ij} \times \vec{p}_i) \cdot (\vec{s}_i + 2\vec{s}_j) \tag{9}$$

is the spin–other-orbit interaction, and $\vec{r}_{ij} = \vec{r}_j - \vec{r}_i$.

Following the inner-projection technique suggested by Rescigno *et al.* [6], the Hamiltonian matrix between two open channels takes the form

$$\langle \psi^{\Omega}_{n_o \ell_o \varepsilon_\nu \ell_\nu(\theta,\beta)} | H | \psi^{\Omega'}_{n'_o \ell'_o \varepsilon'_\nu \ell'_\nu(\theta,\beta')} \rangle = \sum_{n_\nu n'_\nu} O_{\varepsilon_\nu n_\nu} \langle \psi^{\Omega}_{n_o \ell_o n_\nu \ell_\nu} | H | \psi^{\Omega'}_{n'_o \ell'_o n'_\nu \ell'_\nu} \rangle O^t_{n'_\nu, \varepsilon'_\nu}, \tag{10}$$

where the overlap integral

$$O_{\varepsilon_\nu n_\nu} = \langle \psi^{\Omega}_{n_o \ell_o \varepsilon_\nu \ell_\nu(\theta,\beta)} | \psi^{\Omega}_{n_o \ell_o n_\nu \ell_\nu} \rangle \tag{11}$$

and its corresponding transpose

$$O^t_{n'_\nu, \varepsilon'_\nu} = \langle \psi^{\Omega'}_{n_o \ell_o n_{\nu'} \ell_{\nu'}} | \psi^{\Omega'}_{n_o \ell_o \varepsilon'_\nu \ell'_\nu(\theta,\beta')} \rangle. \tag{12}$$

The Hamiltonian matrix between one open and one closed channel can be readily obtained by setting $\theta=0$ and $\beta=0$ in one of the open channels in Eq. (10), i.e.,

$$\langle \psi^{\Omega}_{n_o \ell_o n_\nu \ell_\nu} | H | \psi^{\Omega'}_{n'_o \ell'_o \varepsilon'_\nu \ell'_\nu(\theta,\beta')} \rangle = \sum_{n'_\nu} \langle \psi^{\Omega}_{n_o \ell_o n_\nu \ell_\nu} | H | \psi^{\Omega'}_{n'_o \ell'_o n'_\nu \ell'_\nu} \rangle O^t_{n'_\nu, \varepsilon'_\nu} \tag{13}$$

and

$$\langle \psi^{\Omega}_{n_o \ell_o \varepsilon_\nu \ell_\nu(\theta,\beta)} | H | \psi^{\Omega'}_{n'_o \ell'_o n'_\nu \ell'_\nu} \rangle = \sum_{n_\nu} O_{\varepsilon_\nu n_\nu} \langle \psi^{\Omega}_{n_o \ell_o n_\nu \ell_\nu} | H | \psi^{\Omega'}_{n'_o \ell'_o n'_\nu \ell'_\nu} \rangle. \tag{14}$$

Finally, the Hamiltonian matrix between two closed channels, i.e.,

$$\langle \psi^{\Omega}_{n_o\ell_o n_\nu \ell_\nu} | H | \psi^{\Omega'}_{n'_o\ell'_o n'_\nu \ell'_\nu} \rangle, \tag{15}$$

is calculated using the same procedure for the BSCI method outlined in [1] for the nonrelativistic Hamiltonian H_{nr} and in [18] for the spin-dependent interactions H_m. The configuration mixing between the bound and continuum components of the state functions is accounted for by including all negative and positive energy one-particle orbital functions $\chi_{n_\nu \ell_\nu}$ and $\chi_{n'_\nu \ell'_\nu}$ in the overlap integrals $O_{\varepsilon_\nu n_\nu}$ and $O^t_{n'_\nu, \varepsilon'_\nu}$. For a converged result, the BSCR calculation has shown that the "quasicomplete" set of real functions $\psi^{\Omega}_{n_o\ell_o n_\nu \ell_\nu}$, which satisfy the boundary condition given by Eq. (31) of [1], must cover the energy region of the calculated spectrum. The use of the inner-projection technique, together with the orthonormal sets of orbital functions, makes it easier to characterize the atomic states of interest, especially the spin mixing.

Similar to the procedure proposed earlier by Chang and Bryan [18], the BSCR calculation is also carried out by first diagonalizing the Hamiltonian matrix which includes only the nonrelativistic Hamiltonian H_{nr} corresponding to a set of (SLJ) states using the expressions given by Eqs. (10)–(15). The resulting set of orthogonal energy eigenfunctions (which we shall denote as *zeroth-order-state wave functions* similar to the ones in [18]) is then employed as a set of new basis functions in the construction of the complex matrix for the total Hamiltonian which couples all allowed (SL) states through the spin-dependent interactions H_m. The key advantage of employing the zeroth-order-state wave function is to offer a possibility to effectively identify the degree of mixing of the spin states from the calculated J-dependent state wave functions for each of the atomic resonances.

The diagonalized complex energy $E_\mu(\theta,\beta)=E^\mu_{res}-i\Gamma_\mu/2$ from the nonrelativistic complex Hamiltonian matrix leads to an estimated resonance energy E^μ_{res} and its corresponding resonance width Γ_μ. The variational parameter β for each open channel is determined by the condition

$$\left(\frac{\partial |E_\mu(\theta,\beta)|}{\partial \beta} \right) = 0, \tag{16}$$

where the absolute value indicates that both E^μ_{res} and Γ_μ are optimized simultaneously. Similar to the example shown by Fig. 14 of [2], Fig. 1 presents a typical example of the variations of E_{res} and Γ. The optimal β for the Mg $3p5s\ ^1P$ doubly excited resonance is determined as β varies from 0.31 to 0.39. The success of the BSCR method also depends largely on the stability of the value β as θ varies. It turns out that, in the application of the BSCR approach presented in Sec. III, our estimated β values for all members of an autoionization series vary very little, and can be approximated by a single value for each resonance series. In fact, even for different autoionization series decaying into the same open channel, our calculation has shown that a single β is a reasonably good approximation for each open channel. Once the optimized β value is determined as shown in Fig. 1, θ is varied again to assure the stability of the resonance parameters. We also note that the β parameter in the BSCR approach is similar to the nonlinear parameter of the Slater-type functions

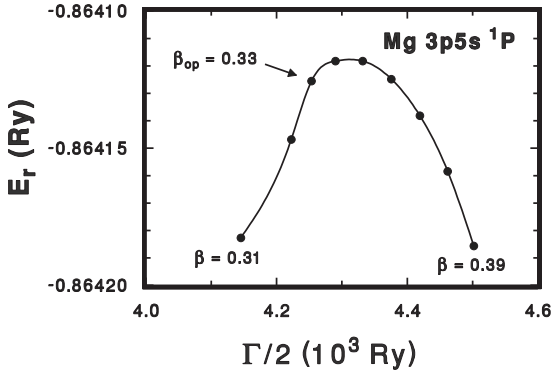

FIG. 1. The variations of E_{res} and Γ of the Mg $3p5s\ ^1P$ resonance as β changes from 0.31 to 0.39. The θ value is stabilized at around 0.32 rad.

used by Davis and Chung [16], or the Hylleraas-type functions used by Ho [14], with the same optimum condition, i.e., Eq. (3.1.2b) of [14].

With the variational parameters properly determined, the energy eigenfunction (i.e., the zeroth-order-state wave function) following the diagonalization of the nonrelativistic complex Hamiltonian matrix may be expressed as the sum of the bound (i.e., all closed channel j) and continuum (i.e., all open channel k) components, i.e.,

$$\phi^{\Omega}_{\mu}(\theta) = \sum_j C^{(SLJ)\mu}_{n'_j\ell'_j n_j \ell_j} \psi^{\Omega}_{n'_j\ell'_j n_j \ell_j} + \sum_k C^{(SLJ)\mu}_{n'_k\ell'_k \varepsilon_k \ell_k(\theta)} \psi^{\Omega}_{n'_k\ell'_k \varepsilon_k \ell_k(\theta,\beta_k)}. \tag{17}$$

The series of doubly excited autoionization resonances $|n_0\ell_0 n_\mu \ell_\mu\rangle$ with an inner electron $n_0\ell_0$ can be identified approximately by projecting the state function $\phi^{\Omega}_{\mu}(\theta)$ to its corresponding basis function $\psi^{\Omega}_{n_0\ell_0 n_\nu \ell_\nu}$, i.e., by calculating the spectral density

$$\rho^{SLJ}_{\mu} = \sum_\nu |\langle \phi^{\Omega}_{\mu}(\theta) | \psi^{\Omega}_{n_0\ell_0\, n_\nu \ell_\nu} \rangle|^2 = \sum_\nu |C^{(SLJ)\mu}_{n_0\ell_0 n_\nu \ell_\nu}|^2. \tag{18}$$

With this choice of zeroth-order-state wave functions as the basis functions, the new Hamiltonian matrix is constructed by including the spin-dependent interactions H_m. Since the nonrelativistic H_{nr} is already diagonalized with respect to the basis functions, no additional calculation is required, i.e.,

$$\langle \phi^{\Omega}_{\mu}(\theta) | H_{nr} | \phi^{\Omega'}_{\nu}(\theta) \rangle = \delta_{\Omega\Omega'} \delta_{\mu\nu} E_\mu(\theta). \tag{19}$$

The Hamiltonian matrix elements for H_m, i.e.,

$$\langle \phi^{\Omega}_{\mu}(\theta) | H_m | \phi^{\Omega'}_{\nu}(\theta) \rangle, \tag{20}$$

are evaluated in terms of the expressions given by Eqs. (10)–(15), with $H=H_m$ and the matrix element $\langle \psi^{\Omega}_{n_o\ell_o n_\nu \ell_\nu} | H_m | \psi^{\Omega'}_{n'_o\ell'_o n'_\nu \ell'_\nu} \rangle$ of Eqs. (9), (A1), and (A8) in [18]. For each total angular momentum J, all allowed SL states are included in the construction of the total Hamiltonian matrix. The energy eigenvalues $E_\mu=E^\mu_{res}-i\Gamma_\mu/2$ and their corresponding state functions

$$\Phi_{\mu}^{JM}(\theta) = \sum_{S,L,\nu} C_{\nu}^{(SL)J\mu} \phi_{\nu}^{\Omega}(\theta) \tag{21}$$

are obtained by diagonalizing the new Hamiltonian matrix using the standard International Mathematical and Statistical Libraries (IMSL) routines for the generalized eigenvalue problem. The mixing of the spin states can be determined by the sum of the squares of the appropriate expansion coefficients, i.e., $|C_{\nu}^{(SL)J\mu}|^2$.

The photoionization cross section $\sigma(E)$ from an initial state $\Phi_I^{J_I M_I}$ with an energy E_I is given by [7]

$$\sigma(E) = 4\pi\alpha f_{EI}, \tag{22}$$

where α is the fine-structure constant and the complex transition amplitude f_{EI} is given by

$$f_{EI} = \frac{(\Delta E)^{\pi_\gamma}}{3g_I} \mathrm{Im}\left(\sum_{\mu} \sum_{q,M,M_I} \frac{\langle \Phi_I^{J_I M_I} | D_q^{[1]} | \Phi_{\mu}^{JM}(\theta) \rangle^2}{E_{\mu}(\theta) - E} \right), \tag{23}$$

where $g_I = 2J_I + 1$ is the degree of degeneracy of the initial state I and $\Delta E = E - E_I$ is the transition energy. The state function of the initial state,

$$\Phi_I^{J_I M_I} = \sum_{S_I, L_I} \sum_{i} C_{n_i' \ell_i' n_i \ell_i}^{(S_I L_I J_I)} \psi_{n_i' \ell_i' n_i \ell_i}^{\Omega_I}, \tag{24}$$

is calculated with the procedure outlined in [1,18].

The cross section $\sigma(E)$ given by Eq. (22) can be readily identified as the *imaginary* part of the dynamic polarizability [14,19,20]. In the length approximation, the dipole operator $D = \hat{\epsilon} \cdot (\vec{r}_1 + \vec{r}_2)$ and $\pi_\gamma = 1$, and in the velocity approximation, $D = \hat{\epsilon} \cdot (\vec{\nabla}_1 + \vec{\nabla}_2)$ and $\pi_\gamma = -1$, where $\hat{\epsilon}$ represents the light polarization. More explicitly,

$$f_{EI} = \frac{(\Delta E)^{\pi_\gamma}}{3g_I} \mathrm{Im}\left(\sum_{\mu} \frac{[F_{EI}^{\mu}(\theta)]^2}{E_{\mu}(\theta) - E} \right), \tag{25}$$

and

$$F_{EI}^{\mu}(\theta) = \sum_{SLS_I L_I \nu i} C_{\nu}^{(SL)J\mu} \left(\sum_{j} C_{n_j' \ell_j' n_j \ell_j}^{(SLJ)\nu} C_{n_i' \ell_i' n_i \ell_i}^{(S_I L_I J_I)} D_{EI}^{ji} + \sum_{k} C_{n_k' \ell_k' \varepsilon_k \ell_k(\theta)}^{(SLJ)\nu} O_{\varepsilon_k n_k} C_{n_i' \ell_i' n_i \ell_i}^{(S_I L_I J_I)} D_{EI}^{ki} \right), \tag{26}$$

where $O_{\varepsilon_k n_k} = \langle \psi_{n_k' \ell_k' \varepsilon_k \ell_k(\theta,\beta)}^{\Omega} | \psi_{n_k' \ell_k' n_k \ell_k}^{\Omega} \rangle$ and D_{EI}^{ji} is the real dipole transition matrix between two basis functions $\psi_{n_j' \ell_j' n_j \ell_j}^{\Omega}$ and $\psi_{n_i' \ell_i' n_i \ell_i}^{\Omega_I}$, given by

$$D_{EI}^{ji} = (-1)^{\ell_j + \ell_j'} g(LSJL_I S_I J_I) [d_{EI}(j'j, i'i) + (-1)^{\Delta_I} d_{EI}(j'j, ii') + (-1)^{\Delta} d_{EI}(jj', i'i) + (-1)^{\Delta_I + \Delta} d_{EI}(jj', ii')], \tag{27}$$

where

$$g(LSJL_I S_I J_I) = \delta_{S_I S} [(2J+1)(2J_I+1)(2L+1)(2L_I+1)]^{1/2} \times (-1)^{1+L} \begin{Bmatrix} L & L_I & 1 \\ J_I & J & S \end{Bmatrix}, \tag{28}$$

$$\Delta_I = \ell_i' + \ell_i - L_I - S_I, \tag{29}$$

and

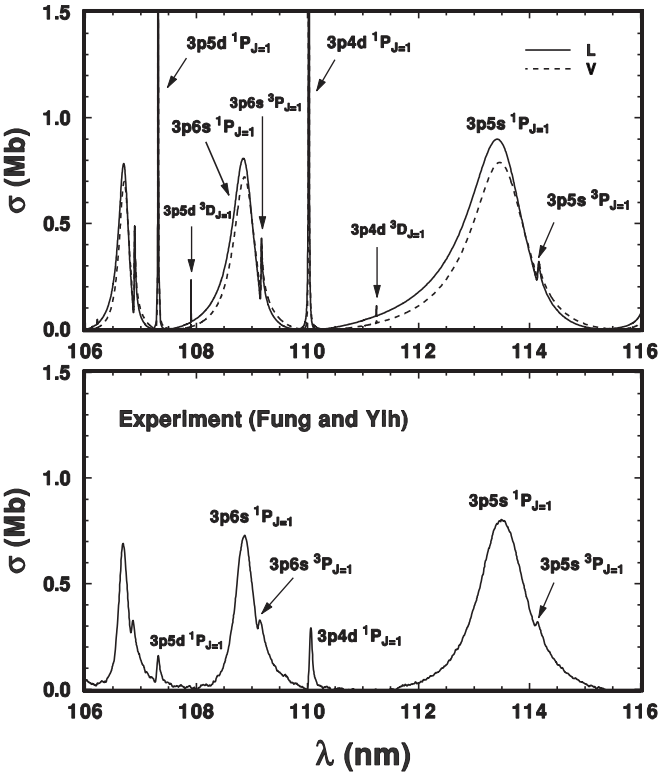

FIG. 2. Comparison between the calculated Mg ground-state photoionization cross sections and the experimentally observed spectrum [22].

$$\Delta = \ell_j' + \ell_j - L - S. \tag{30}$$

For a configuration corresponding to two equivalent electrons, a factor of $1/\sqrt{2}$ should be added. The dipole matrix element d_{EI} is given by Eq. (45) of [1].

III. RESULTS AND DISCUSSION

Some of the earlier BSCI results on Mg, with no spin mixing, are already in good agreement with the experimental and other earlier theories and are presented elsewhere [21]. Figure 2 compares the current results of the spin-mixed BSCR calculation on the Mg ground-state photoionization spectrum with the observed absolute photoabsorption cross sections by Fung and Yih [22]. We should point out that the comparison between theory and experiment for photoabsorption spectra for narrow resonances (e.g., the $3pnd\ ^{1,3}P$ resonances) requires detailed information on (i) the experimental energy resolution, (ii) the detailed characteristic of the slit function for the incident light, and (iii) the vapor density of the medium [23]. In the absence of these detailed experimental parameters, to compare with the observed spectra, a convoluted theoretical spectrum for a narrow resonance would have three free parameters to adjust the peak cross sections. As a result, the theoretical data could easily be manipulated and artificially matched with the experimental peak cross sections. The theoretical spectrum shown in Fig. 2 represents the calculated BSCR results without the convolution, and the peak cross sections for the narrow resonances, as expected,

TABLE I. Widths (in $a[b]=a\times10^{-b}$ Ry) and resonance energies (in terms of effective quantum number ν against the Mg $3p$ threshold) for $^3P_{J=0,1,2}$ autoionization series.

^3P_J	$J=0$		$J=1$		$J=2$	
	Γ (Ry)	ν	Γ (Ry)	ν	Γ (Ry)	ν
$3p4s$	4.6[−4]	2.323	4.7[−4]	2.323	4.6[−4]	2.323
$3p5s$	2.3[−4]	3.359	2.7[−4]	3.359	2.3[−4]	3.359
$3p6s$	9.5[−5]	4.380	1.8[−4]	4.378	9.5[−5]	4.379
$3p7s$	6.3[−5]	5.401	2.3[−4]	5.394	6.3[−5]	5.401
$3p3d$	1.1[−3]	2.877	1.1[−3]	2.878	1.1[−3]	2.878
$3p4d$	3.3[−4]	3.860	3.1[−4]	3.862	3.1[−4]	3.863
$3p5d$	8.8[−5]	4.855	6.4[−5]	4.866	6.5[−5]	4.867
$3p6d$	4.6[−5]	5.855	2.8[−5]	5.882	2.9[−5]	5.883

are substantially higher than the experimental values. Following our discussion in Sec. II, the optimized values of $\theta=0.32$ rad and $\beta=0.33$ are used in the present calculation.

For Mg, the spin-dependent interaction is not expected to contribute significantly. In the present calculation, for simplicity, we have included only the spin-orbit interaction. Our calculated cross sections quantitatively reproduce very well the experimental data. In addition to the $3pns\ ^{1,3}P_1$ and $3pnd\ ^1P_1$ resonance series, the $3pnd\ ^3D_1$ autoionization series has also been identified in our calculated spectrum, although it is much too small in magnitude to be observed experimentally. The $3pnd\ ^3P_1$ series is both too narrow and too weak to appear in the spectrum shown. The calculated widths and resonance energies (in terms of the effective quantum number ν against the Mg $3p$ threshold) are tabulated in Tables I–III. As expected, the width of the $3pnl\ ^{1,3}P_J$ resonance, which measures qualitatively the interaction strength of the Coulomb interaction between the dominant doubly excited electronic configuration (e.g., $3pns$ or $3pnd$) and the $3s\epsilon p\ ^{1,3}P_J$ continua, decreases as ν increases along the autoionization series, except for the $3p7s\ ^3P_{J=1}$ resonance shown in Table I. It turns out that, in the absence of spin-orbit interaction, the calculated width ($\Gamma=9.5\times10^{-5}$ Ry) of the $3p6s\ ^3P_{J=1}$ resonance is indeed greater than the calculated width ($\Gamma=6.4\times10^{-5}$ Ry) of the $3p7s\ ^3P_{J=1}$ resonance. The widths of both resonances increase substantially when the spin-orbit interaction is included to account for the mixing with the corresponding neighboring and much broader $3pns\ ^1P_{J=1}$ resonances, and the effect on width due to the mixing of spin states is much bigger for the $3p7s\ ^3P_{J=1}$ resonance than that for the $3p6s\ ^3P_{J=1}$ resonance. For the $3pnd\ ^{1,3}D_J$ resonance, it is allowed, in theory, to autoionize into the $3s\epsilon p\ ^{1,3}P_J$ ionization channel only through its small $3pnd\ ^{1,3}P_J$ mixing due to the spin-dependent interactions. As a result, qualitatively, its autoionization width does not have to vary similarly to that of the $3pnl\ ^{1,3}P_J$ resonance as ν increases.

The difference in length and velocity results can be attributed to the use of a model potential [1,13,18], that simulates the polarization of the atomic core. In a separate recent study on oscillator strength for transitions in Be-like systems [24], we succeeded in reducing the difference between length and velocity results by replacing the model potential in our calculation with electronic configurations corresponding to three excited atomic orbitals (i.e., with one of the inner-shell electrons also in an excited orbital). The use of a basis set with atomic orbitals corresponding to three actively interacting electrons accounts explicitly for the polarization of the atomic core. Such calculations, of course, are computationally highly intensive. In general, they do not lead to a different physical interpretation of the atomic transition, except for transitions with extremely small transition rates.

By including the spin-dependent interactions explicitly, the BSCR method offers the possibility of studying directly in a single calculation the spectra leading to autoionization series of various combinations of $[(l_1l_2)LSJ]$. We present in

TABLE II. Widths (in $a[b]=a\times10^{-b}$ Ry) and resonance energies (in terms of effective quantum number ν against the Mg $3p$ threshold) for $^3D_{J=1,2}$ autoionization series.

^3D_J	$J=1$		$J=2$	
	Γ (Ry)	ν	Γ (Ry)	ν
$3p3d$	4.5[−6]	2.821	5.1[−6]	2.821
$3p4d$	2.7[−5]	3.829	2.8[−5]	3.829
$3p5d$	2.4[−5]	4.823	2.8[−5]	4.826
$3p6d$	1.9[−5]	5.811	2.6[−5]	5.821

TABLE III. Widths (in $a[b]=a\times10^{-b}$ Ry) and resonance energies (in terms of effective quantum number ν against the Mg $3p$ threshold) for $^1P_{J=1}$ and $^1D_{J=2}$ autoionization series.

	$^1P_{J=1}$		$^1D_{J=2}$	
	Γ (Ry)	ν	Γ (Ry)	ν
$3p4s$	3.06[−2]	2.399		
$3p5s$	8.47[−3]	3.438		
$3p6s$	3.33[−3]	4.451		
$3p7s$	1.55[−3]	5.466		
$3p3d$	2.1 [−4]	3.111	1.0[−5]	2.564
$3p4d$	6.4 [−5]	4.108	7.0[−5]	3.632
$3p5d$	2.5 [−5]	5.109	1.2[−4]	4.657
$3p6d$	6.7 [−6]	6.118	1.0[−4]	5.675

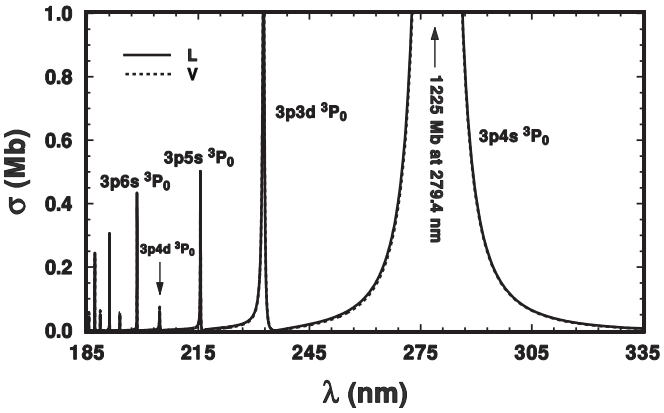

FIG. 3. Calculated photoionization spectrum from the Mg metastable $3s4s\ ^3S_{J=1}$ state to the $J=0$ continuum.

Figs. 3–5 the calculated photoionization spectra from the Mg metastable $3s4s\ ^3S_{J=1}$ state to $J=0,1,2$ final continua. For the $J=0$ continuum, only two odd-parity autoionization series, i.e., a stronger $3pns\ ^3P_0$ series and a weaker $3pnd\ ^3P_0$ series, are allowed. As expected, the spectrum shown in Fig. 3 is dominated by the shakeup of an outer $4s$ electron following the one-electron inner $3s \rightarrow 3p$ core excitation [25]. The length and velocity results agree very well. For the $J=2$ continuum, all four allowed autoionization series, i.e., $3pns\ ^3P_2$, $3pnd\ ^3P_2$, and $3pnd\ ^{1,3}D_2$ series, are identified in Fig. 4. Again, the spectrum is dominated by the shakeup of the outer $4s$ electron with a peak cross section over 6000 Mb. As expected, the transitions to the spin-flip $3pnd\ ^1D_2$ resonances are very weak.

For the $J=1$ continuum, there are a total of five allowed odd-parity autoionization series, i.e., the $3pns\ ^{1,3}P_1$, $3pnd\ ^{1,3}P_1$, and $3pnd\ ^3D_1$ series. Similar to the $J=0$ and 2 spectra, the $J=1$ spectrum is dominated by the $3p4s\ ^3P_1$ resonance due to the shakeup of the outer $4s$ electron following the inner $3s \rightarrow 3p$ core excitation. The rest of the $3pns\ ^3P_1$ resonances can also be clearly identified, as shown in Fig. 5. The pair of $3pnd\ ^3P_1$ series (on the shorter-wavelength, or higher-energy, side) and $3pnd\ ^3D_1$series (on the longer-wavelength side) are also clearly shown. The transition rate to the $3pnd\ ^1P_1$ series is expected to be very

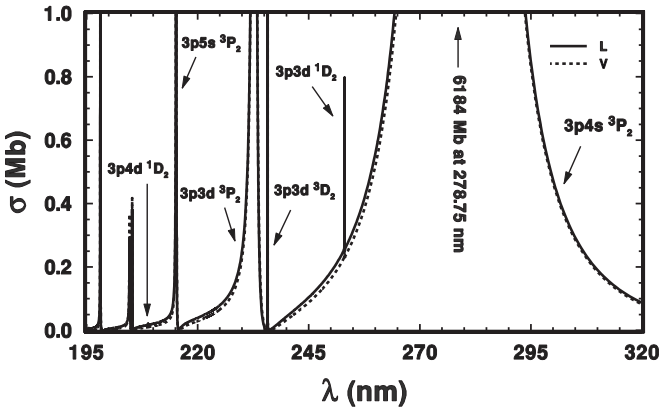

FIG. 4. Calculated photoionization spectrum from the Mg metastable $3s4s\ ^3S_{J=1}$ state to the $J=2$ continuum.

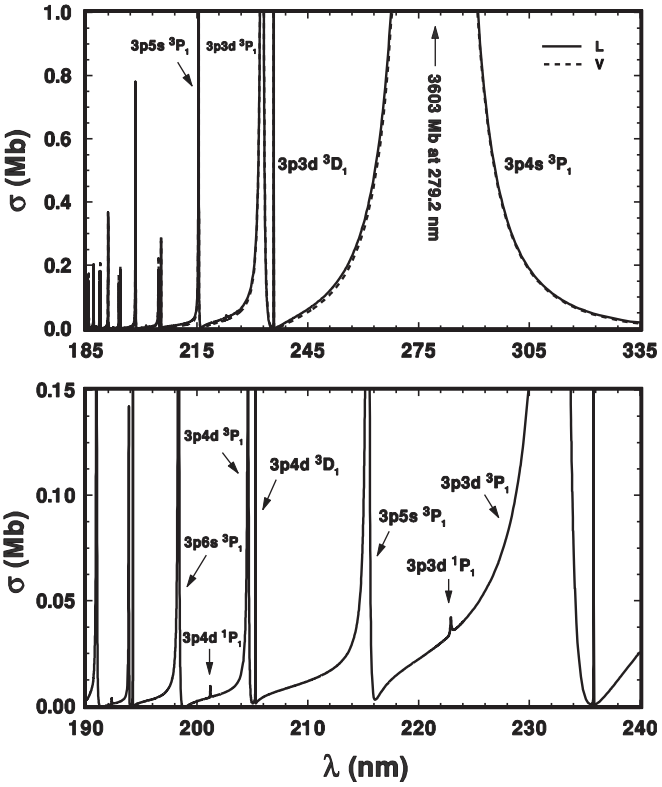

FIG. 5. Calculated photoionization spectrum from the Mg metastable $3s4s\ ^3S_{J=1}$ state to the $J=1$ continuum.

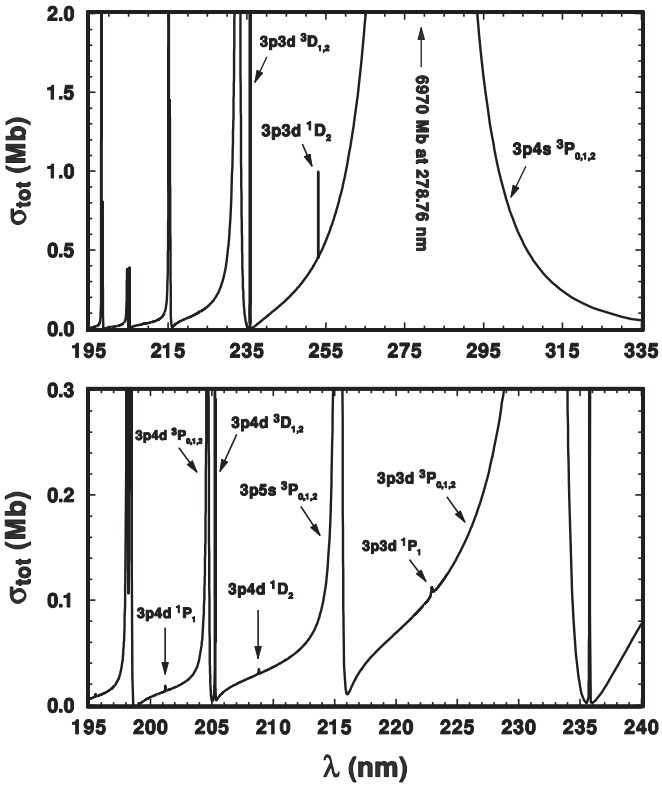

FIG. 6. Calculated total photoionization spectrum from the Mg metastable $3s4s\ ^3S_{J=1}$ state to $J=0,1$, and 2 continua.

small, due to the spin flip and the change of electronic orbitals of both outer electrons. As a result, the $3pnd\ ^1P_1$ resonances barely show up in our calculated spectrum shown in Fig. 5. We also find with interest that the relatively broad $3pns\ ^1P_1$ series, i.e., the one that dominates the ground-state spectrum shown in Fig. 2, does not appear in the $J=1$ spectrum from the metastable $3s4s\ ^3S_1$ state shown in Fig. 5. Of course, the transition rate to the spin-flip $3pns\ ^1P_1$ series is expected to be small due to the change of spin, similar to the ionization leading to the $3pnd\ ^1P_1$ and $3pnd\ ^1D_2$ series. But why should a substantially broader $3p4s\ ^1P_1$ resonance fail to show up, whereas the spin-flip $3pnd\ ^1P_1$ resonances can be seen in our calculated spectrum? This can be readily attributed to the fact that the weak transition rate to the spin-flip $3p4s\ ^1P_1$ resonance is overshadowed by the fairly large $3p4s\ ^3P_1$ cross sections extended over a large energy region (much larger than its width) with a peak cross section over 3000 Mb. The total photoionization cross sections, including transitions to all continua, are given in Fig. 6.

Whereas the other *B*-spline-based approaches offer advantages in computational efficiency, the BSCR method presented in this paper, with the spin-dependent interactions explicitly included, offers an alternative to investigate in detail the configuration mixing in the spectral density of doubly excited resonances embedded in multiple continua through Eqs. (17) and (18), and also the mixing of the spin states through Eq. (21).

ACKNOWLEDGMENTS

This work was supported by the National Science Council in Taiwan under NSC Grants No. 95-2119-M-007-001, No. 94-2112-M-030-002, and No. 92-2811-M-008-035.

[1] T. N. Chang, in *Many-body Theory of Atomic Structure and Photoionization*, edited by T. N. Chang (World Scientific, Singapore, 1993), p. 213.
[2] T. N. Chang and T. K. Fang, Radiat. Phys. Chem. **70**, 173 (2004).
[3] T. K. Fang and T. N. Chang, Phys. Rev. A **61**, 062704 (2000).
[4] H. S. Fung, H. H. Wu, T. S. Yih, T. K. Fang, and T. N. Chang, Phys. Rev. A **64**, 052716 (2001).
[5] T. K. Fang and Y. K. Ho, Phys. Rev. A **60**, 2145 (1999); Y. K. Ho and T. K. Fang, J. Chin. Chem. Soc. (Taipei) **48**, 539 (2001).
[6] T. N. Rescigno, C. W. McCurdy, Jr., and A. E. Orel, Phys. Rev. A **17**, 1931 (1978); T. N. Rescigno and C. W. McCurdy, *ibid.*, **31**, 624 (1985).
[7] T. N. Rescigno, Phys. Rev. A **31**, 607 (1985).
[8] C. W. McCurdy, M. Baertschy, and T. N. Rescigno, J. Phys. B **37**, R137 (2004); C. W. McCurdy and F. Martin, *ibid.* **37**, 917 (2004).
[9] C. de Boor, *A Practical Guide to Splines* (Springer-Verlag, New York, 1978).
[10] W. Vanroose, D. A. Horner, F. Martin, T. N. Rescigno, and C. W. McCurdy, Phys. Rev. A **74**, 052702 (2006); W. Vanroose, F. Martin, T. N. Rescigno, and C. W. McCurdy, *ibid.* **70**, 050703(R) (2004).
[11] H. Bachau, E. Cormier, P. Decleva, J. E. Hansen, and F. Martin, Rep. Prog. Phys. **64**, 1815 (2001).
[12] J. L. Sanz-Vicario, E. Lindroth, and N. Brandefelt, Phys. Rev. A **66**, 052713 (2002).
[13] L. A. A. Nikolopoulos, Phys. Rev. A **71**, 033409 (2005).
[14] Y. K. Ho, Phys. Rep. **99**, 1 (1983).
[15] T. K. Fang, Y. K. Ho, and Y. C. Lin, in *Proceedings of the International Seminar on Photoionization in Atoms*, edited by Y. Azuma *et al.* (Kyoto University Press, Kyoto, 2002), p. 12.
[16] B. F. Davis and K. T. Chung, Phys. Rev. A **36**, 1948 (1987).
[17] H. A. Bethe and E. E. Salpeter, *Quantum Mechanics of One- and Two-electron Atoms* (Springer-Verlag, Berlin, 1957).
[18] T. N. Chang and E. T. Bryan, Phys. Rev. A **38**, 645 (1988).
[19] U. Fano and J. W. Cooper, Rev. Mod. Phys. **40**, 441 (1968).
[20] H. P. Kelly and A. Ron, Phys. Rev. A **5**, 168 (1972).
[21] T. N. Chang and X. Tang, Phys. Rev. A **46**, R2209 (1992); T. K. Fang and Y. K. Ho, Chin. J. Phys. (Taipei) **37**, 37 (1999).
[22] H. S. Fung and T. S. Yih, Nucl. Phys. A **684**, 696c (2001).
[23] T. K. Fang and T. N. Chang, Phys. Rev. A **57**, 4407 (1998); R. D. Hudson and V. L. Carter, J. Opt. Soc. Am. **58**, 227 (1968); W. F. Chan, G. Cooper, and C. E. Brion, Phys. Rev. A **44**, 186 (1991); T. N. Chang, Y. Luo, H. S. Fung, and T. S. Yih, J. Chin. Chem. Soc. (Taipei) **48**, 347 (2001).
[24] T. N. Chang and Y. Luo, J. Phys.: Conf. Ser. (to be published); Yuxiang Luo, Ph.D. dissertation, University of Southern California, 2007.
[25] T. K. Fang, B. I. Nam, Y. S. Kim, and T. N. Chang, Phys. Rev. A **55**, 433 (1997).